Steel and Composite Structures, *Vol. 21, No. 3 (2016) 501-515*
DOI: http://dx.doi.org/10.12989/scs.2016.21.3.501

Seismic analysis of steel structure with brace configuration using topology optimization

Shengfang Qiao [1a], Xiaolei Han [*1], Kemin Zhou [2a] and Jing Ji [1a]

[1] *School of Civil Engineering and Transportation, South China University of Technology, Tianhe, Guangzhou, 510641, China*
[2] *College of Civil Engineering, Huaqiao University, Jimei, Xiamen, 361021, China*

(*Received December 08, 2015, Revised April 06, 2016, Accepted May 06, 2016*)

Abstract. Seismic analysis for steel frame structure with brace configuration using topology optimization based on truss-like material model is studied. The initial design domain for topology optimization is determined according to original steel frame structure and filled with truss-like members. Hence the initial truss-like continuum is established. The densities and orientation of truss-like members at any point are taken as design variables in finite element analysis. The topology optimization problem of least-weight truss-like continuum with stress constraints is solved. The orientations and densities of members in truss-like continuum are optimized and updated by fully-stressed criterion in every iteration. The optimized truss-like continuum is founded after finite element analysis is finished. The optimal bracing system is established based on optimized truss-like continuum without numerical instability. Seismic performance for steel frame structures is derived using dynamic time-history analysis. A numerical example shows the advantage for frame structures with brace configuration using topology optimization in seismic performance.

Keywords: brace; topology optimization; truss-like; story drift; dynamic time-history analysis

1. Introduction

Seismic rehabilitation for existing building has been emphasized in recent years. ASCE (2013) issued the latest standard for seismic evaluation and renovation of new and existing buildings. Brace is an effective way to reinforce structures. Tasbihgoo *et al*. (2009) employed brace to reinforce Santa Monica Place Mall according to ASCE41 (2006). D'Aniello *et al*. (2013) studied the seismic performance of steel frames with concentric braces by numerical simulation. Rezvani and Asgarian (2014) suggested the level against progressive collapse for frame can be enhanced by concentrical braces. Some advantages of brace under the quasi-static cyclic test were presented by Jia *et al*. (2014). Ghowsi and Sahoo (2015) studied the effect of near-field earthquakes on fragility of braced frame. The high strength steel combination was introduced for braced frame by Lian *et al*. (2015). The seismic resilience of braced frame was discussed using incremental dynamic analysis by Tirca *et al*. (2015). In order to improve the performance of braced frames, suspended zipper bracing system is demonstrated by Abdollahzadeh and Abbasi (2015). A new brace

*Corresponding author, Professor, E-mail: xlhan@scut.edu.cn
[a] Ph.D. Student, E-mail: sfqiao@yahoo.com

http://www.techno-press.org/?journal=scs&subpage=6 ISSN: 1229-9367 (Print), 1598-6233 (Online)

configuration was studied for reinforced concrete frames by Qu *et al*. (2015). Most researches concerned the anti-seismic property of brace and most brace configurations were adopted by engineering experiences, however, the reasonable brace configuration was not highlighted similarly.

Luckily, brace configuration can be established by employing structural topology optimization. Bendsøe and Kikuch (1988) established optimal topologies using a homogenization method which aims to suppress the intermediate density. A simple procedure was presented by Xie and Steven (1993), which is to delete elements with minor density for topology optimization directly. Optimal brace configuration has been concerned by topology optimization. Mijar *et al*. (1998) demonstrated the initial configuration of frame bracing systems can be established by structural topology optimization. Liang *et al*. (2000) argued the topology optimization by Xie and Steven (1993) is an effective way to establish reasonable configuration for bracing systems. Zhu *et al*. (2014) discussed the optimized structure with constructability considered. Aydin *et al*. (2015) discussed the distribution of steel diagonal braces by the optimization method. Lee *et al*. (2015) introduced the newly conceptual design method for tall buildings under lateral loads using topology optimization. However, the numerical instabilities are showed in most optimized results because of deleting elements or suppressing intermediate density. Further, the seismic response is not discussed in most researches.

Zhou and Li (2005) presented a new method for continuum topology optimization using a truss-like material model. Since intermediate density is not restrained in the iterative process of truss-like material model, the numerical instabilities are avoided. Zhou and Chen (2014) derived the optimized configuration for bracing system based on truss-like material model with natural frequency constrains. However, load patterns cannot be considered for optimized configuration with natural frequency constrains. In this paper, brace configuration is mainly studied under earthquake load (or wind load) by topology optimization using truss-like material model with stress constrains. The optimized brace configuration is derived under minor earthquake when beams, columns and braces are in the elastic phase, nevertheless, structures often yield under strong earthquakes. In order to employ brace configuration based on topology optimization reliably, seismic analysis is also beneficial to be studied. Moreover, seismic analysis is conducted and elastic-plastic material model is employed in software Perform-3D (2008).

2. The procedure of seismic performance assessment for steel frame structure with optimized bracing system

2.1 Information of original frame structure

In order to reinforce an original frame structure, detailed information is necessary, including size, shape and so on. The initial domain of topology optimization is established according to the features of original frame structure.

2.2 The topology optimization method based on truss-like material model under minor earthquake

The initial domain is divided by finite element mesh and full of truss-like material. The truss-like members at any node of elements are presented while members inside the elements are not showed, which are demonstrated in Fig. 1(a). The densities and directions of two orthogonal members at any node j can be expressed as t_{1j}, t_{2j} and α_j, $\alpha_j + \pi/2$ in Fig. 1(b) respectively. Further, densities and orientation of any node j are taken as design variables during finite element analysis. Elastic matrix of global coordinate system can be represented as

$$\boldsymbol{D}(t_1, t_2, \alpha) = E\sum_{b=1}^{2} t_{bj} \sum_{r=1}^{3} s_{br} g_r(\alpha_j)\boldsymbol{A}_r \tag{1}$$

Where, r = 1, 2, 3, b = 1, 2, s_{br}, g_r and A_r were introduced in Zhou and Chen (2014). Moreover, elastic matrix of any point within the elements can be obtained by interpolation.

$$\boldsymbol{D}_e(\xi,\eta) = \sum_{j\in S_e} N_j(\xi,\eta)\boldsymbol{D}_j = E\sum_{j\in S_e} N_j(\xi,\eta)\sum_{b=1}^{2} t_{bj} \sum_{r=1}^{3} s_{br} g_r(\alpha_j)\boldsymbol{A}_r \tag{2}$$

According to the definition of the element stiffness matrix in finite element method

$$\boldsymbol{k}_e = \int_{V_e} \boldsymbol{B}^{\mathrm{T}}\boldsymbol{D}\boldsymbol{B}\,\mathrm{d}V = \sum_{j\in S_e}\sum_{b} t_{bj}\sum_{r} g_r(\alpha_j)\boldsymbol{H}_{ejr} \tag{3}$$

B denotes geometric matrix. Where

$$\boldsymbol{H}_{ejr} = E\int_{V_e} N_j \boldsymbol{B}^{\mathrm{T}}\boldsymbol{A}_r\boldsymbol{B}\,\mathrm{d}V \tag{4}$$

Design variables are not contained in Eq. (4). So it is constant matrix in regular elements. Total finite element stiffness matrix can be formed by assembling Eq. (3).

$$\boldsymbol{K} = \sum_{e} \boldsymbol{k}_e \tag{5}$$

The equation of finite element analysis can be written as

$$\boldsymbol{KU} = \boldsymbol{F} \tag{6}$$

F represents force vector under minor earthquake and U denotes displacement vector in nodes accordingly. By solving finite element Eq. (6), strain can be derived.

$$\boldsymbol{\varepsilon} = \boldsymbol{BU} = \boldsymbol{BK}^{-1}\boldsymbol{F} \tag{7}$$

U_e stands for the displacement vector of element. Stress can be expressed as

$$\boldsymbol{\sigma} = \boldsymbol{DBU}_e \tag{8}$$

$\sigma_j = [\sigma_{xj} \quad \sigma_{yj} \quad \sigma_{xyj}]$ for every node j in Eq. (8). The principal stress direction can be gained as

$$\alpha_j = \frac{1}{2}\arctan\frac{\tau_{xyj}}{\sigma_{xj} - \sigma_{yj}} \tag{9}$$

(a) Initial domain (b) Node "*j*"

Fig. 1 Truss-like material model

Further, principal stress can be obtained

$$\sigma_{1j,2j} = \frac{\sigma_{xj} + \sigma_{yj}}{2} \pm \sqrt{(\frac{\sigma_{xj} - \sigma_{yj}}{2})^2 + \frac{\tau_{xyj}^2}{4}} \tag{10}$$

The two orthogonal truss-like members are arranged along the principal stress directions. Furthermore, the densities of two orthogonal truss-like members can be acquired and updated by full stress criterion. The optimized analysis is conducted in complete elasticity state. Hence, the elastic-plastic material model is not considered under minor earthquake.

$$\begin{aligned} & t_{bjl}^{i+1} = \max(\underline{t}, t_{bjl}^{i} \sigma_{bjl}^{i} / \sigma_p), \\ & (b = 1,2; j = 1,2 \cdots n; l = 1,2 \cdots L) \end{aligned} \tag{11}$$

i represents iterations. t is the minimum density limits (avoiding stiffness matrix singular). σ_p denotes yielding stress. The value of biggest change is represented as

$$\delta = \max_{\substack{b=1,2 \\ j=1,2\cdots n}} \left| \frac{t_{bj}^{i+1} - t_{bj}^{i}}{t_{bj}^{i}} \right| \tag{12}$$

If $\delta \leq 1\%$, this analysis is completed and optimal truss-like continuum is established. Finally, the brace configuration for frame structure is obtained according to the optimal truss-like continuum.

2.3 Seismic performance analysis

Seismic analysis of frame structures are simulated by dynamic time-history analysis based on software Perform-3D.

3. Numerical examples

3.1 Engineering information

The plan of 10-storey original regular steel structure is presented in Fig. 2(a). Hence 2D frame can be used in Fig. 2(b). I section information for columns and beams are shown in Table 1, which

Table 1 Member section for every storey (mm)

Columns for 1-3 storey*	Columns for 4-7 storey	Columns for 8-10 storey	Beams for 1-10 storey
400×400×14×12	350×400×12×10	300×400×10×8	200×450×12×10

*width×height×flap thickenss×Web thickness of I section for 1-3 storey column

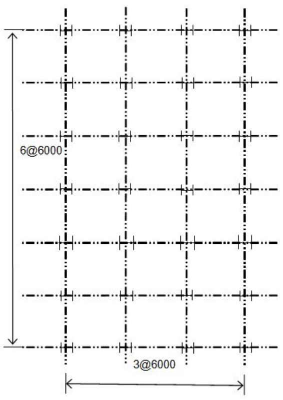

(a) Structure plan

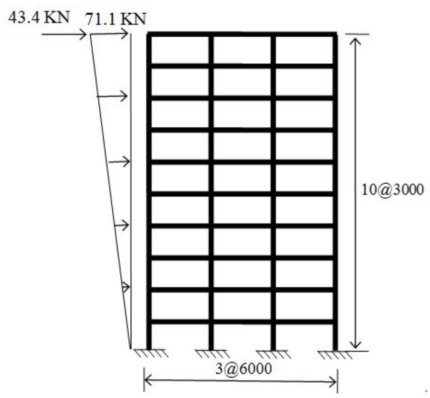

(b) Structure facade

Fig. 2 Structure diagram(mm)

is demonstrated in Fig. 2(b). This building is located at 8 degree protected earthquake intensity (peak earthquake acceleration is 0.40 g for rare earthquake), and site predominant period is 0.35 s based on GB50011 (2010). Thus, seismic action can be calculated under minor earthquake. Further, inverted triangular horizontal load is presented in Fig. 2(b), which is formed based on GB50011 (2010). Higher mode effects are also taken in consideration using additional force on the top storey in Fig. 2(b).

3.2 Topology optimization analysis based on truss-like material model

3.2.1 Topology optimization analysis for integral structure

The initial domain of integral structure is presented in Fig. 3(a). The number of finite element mesh is 240 in initial domain, as shown in Fig. 3(a). The initial density and direction of nodes are assigned, which are also demonstrated in Fig. 3(a). While the members inside elements are not presented. The length and direction of lines at any node denote the density and direction of two orthogonal truss-like members respectively. The members inside the elements can be obtained by interpolated function. Young's modulus E is 206 Gpa. Allowable stress is 235 Mpa. The optimal truss-like continuum is gained by iterations, which is demonstrated in Fig. 3(b). The optimal configuration is established and illustrated in Fig. 3(c) by obtaining truss from truss-like continuum method, which can be found in Zhou and Chen (2014). The braces should not be arranged in the middle of columns, whereas, the braces can be in the middle of beams like diagonal brace or inverted "V" brace in AISC341-10 (2010). In order to construct easily, the modified brace configuration is presented by combining nodes which are close to beam-column joints in Fig. 3(d). However, the building function requirements are not considered in Figs. 3(a)-(d). Further, the braces can be added according to actual engineering requirements. For instance, braces

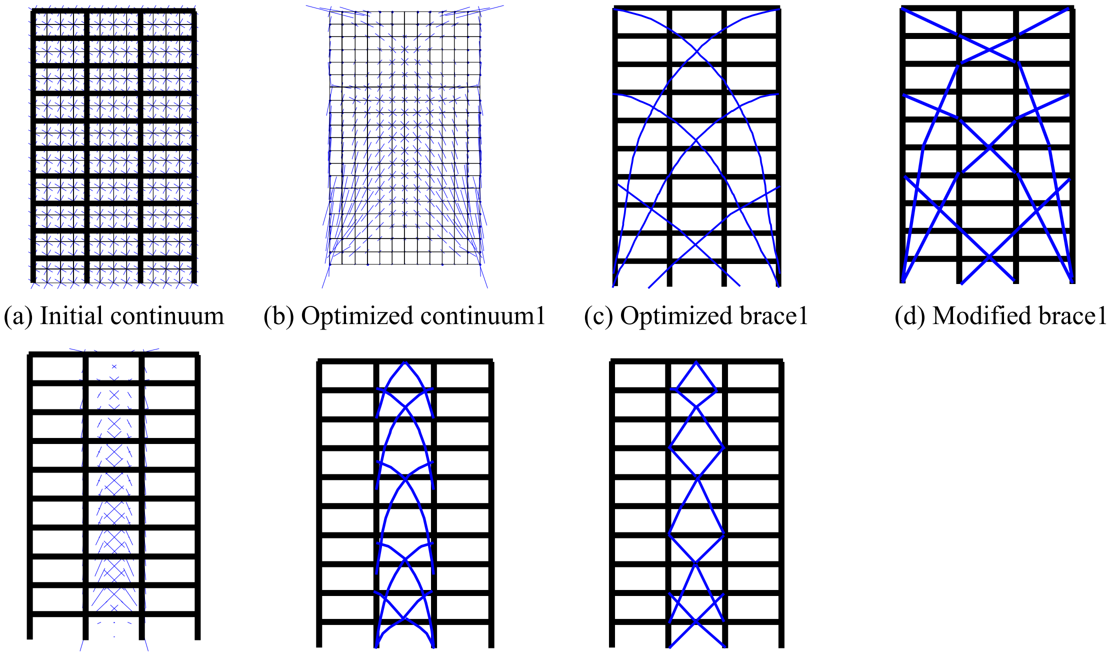

(a) Initial continuum (b) Optimized continuum1 (c) Optimized brace1 (d) Modified brace1

(e) Continuum 2 (f) Optimized brace 2 (g) Modified brace 2

Fig. 3 Optimized analysis for integral structure

only can be installed in the second bay, hence, optimal brace configuration is presented in Figs. 3(e)-(g). Certainly, the optimal configuration should be adopted based on actual structure requirements. The braces above or below the beams can be connected in the top or down surfaces of beams in practice.

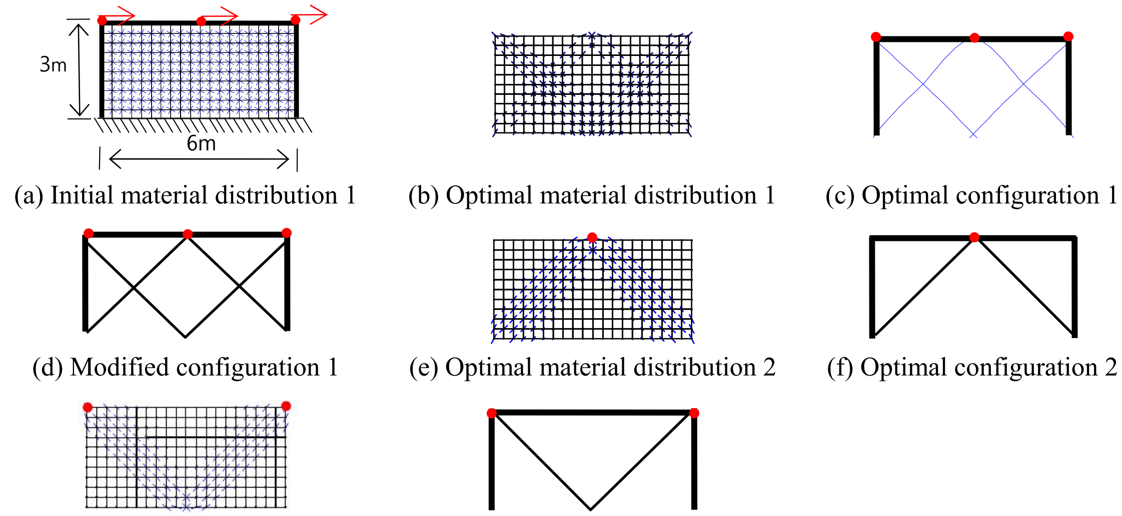

(a) Initial material distribution 1 (b) Optimal material distribution 1 (c) Optimal configuration 1

(d) Modified configuration 1 (e) Optimal material distribution 2 (f) Optimal configuration 2

(g) Optimal material distribution 3 (h) Optimal configuration 3

Fig. 4 Optimized analysis for one-story one-span structure

3.2.2 Topology optimization analysis for one-story one-span structure

Given the actual requirements, brace is sometimes just implemented within one-story one-span space respectively. The topology optimization of one-story one-span structure is presented here, which is flexible to satisfy engineering needs. The number of finite element mesh is 200 in initial domain, as shown in Fig. 4(a). The optimized configuration is established by the method mentioned above, which is demonstrated in Figs. 4(b)-(d). Similarly, optimized brace configuration with only one horizontal concentrated force at the midspan is derived in Figs. 4(e) and (f). Brace configuration with two horizontal concentrated force is depicted in Figs. 4(g) and (h). The optimized configuration in Fig. 4(f) is founded by common inverted "V" employed in Zhu *et al*. (2014) while the configuration in Fig. 4(h) is common "V" brace.

3.2.3 Topology optimization analysis with different storey height

In order to study whether optimized brace configuration is related to the storey height under invariable span, topology optimization analysis with different storey height is discussed. The optimized brace configuration with only one concentrated force is derived in Figs. 5(a)-(c) when the storey height is 6 m. Similarly the optimized configuration with two horizontal concentrated force at the beam-column junction is demonstrated in Figs. 5(d) and (e) when the height is 6 m. Hence the different optimal results can be established according to the different storey height. "X" brace can be derived under pure shear stress state in Fig. 5(f).

The optimal results mentioned above can also demonstrate that the optimal bracing system is established based on truss-like material model without numerical instability. The aforementioned optimal results can also give more details than Mijar *et al*. (1998) and Liang *et al*. (2000). The common "X" brace and common inverted "V" brace are not optimal here, which can be optimized

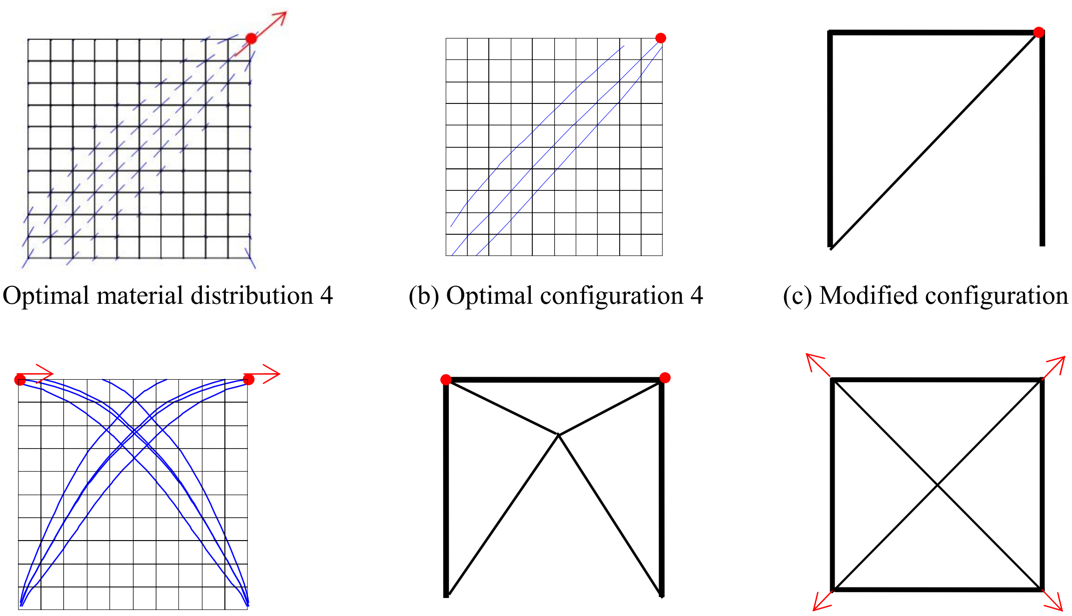

(a) Optimal material distribution 4 (b) Optimal configuration 4 (c) Modified configuration 4

(d) Optimal configuration 5 (e) Modified configuration 5 (f) "X" brace configuration

Fig. 5 Optimized analysis for one-story one-span structure under prescriptive condition and also found in Zhou and Chen (2014). Moreover, the inverted “V” or “V” brace is more acceptable than the single-bar brace when span is twice as much as story height within every bay.

3.3 Seismic performance analysis

3.3.1 Optimized brace distribution

Optimized brace distribution is established according to the optimized brace configuration mentioned above. The optimized brace distribution for integral structure is illustrated in Fig. 6(a). In order to confirm the advantage of optimized configuration, two common brace configurations which are optimized under prescriptive condition mentioned above are employed for comparison in Figs. 6(b)-(c).

Table 2 Material volume (m^3)

Brace configuration	Topology optimization	Inverted “V”	Single-bar	Original frame
Area (mm^2)	1640	1600	2020	--
Total length (m)	165.3	169.7	134.2	--
Total volume (m^3)	0.271	0.271	0.271	3.104

Table 3 Earthquakes

Name	Abbreviation	Duration (s)
Eicentor E-W	E1	10
Eicentor N-S	E2	10
Northridge E-W	E3	10
Northridge N-S	E4	10
Loma Prieta	E5	10
Artificial 1	E6	10
Artificial 2	E7	10

Table 4 Peak ground acceleration (cm/s^2)

Magnitude	Minor earthquake	Rare earthquake
Peak ground acceleration	70	400
Probability of Exceedance (50 years)	63.2%	2%
Damp ratio	0.04	0.05

Table 5 Comparison for the first three periods of original frame

Software	Perform-3D	Opensees	Deviation
First period (s)	2.57	2.64	2.7%
Second period (s)	0.86	0.87	1.1%
Third period (s)	0.49	0.50	2.0%

The additional flexural demand caused by brace on beams and columns are also highlighted herein, hence, braces are designed according to AISC341-10 (2010). Inverted-V brace is adopted as follows

$$V_{\mathrm{u}} = 2A_{brace}f_y \cos\theta \tag{13}$$

Where, A_{brace} and f_y denote the maximum cross-section area and yielding stress of brace. V_u is the shear capacity of steel beam and θ is the angle between beam and brace. The maximum cross-section area is

$$A_{brace} = \frac{V_{\mathrm{u}}}{2f_y \cos\theta} \qquad (\theta = 45^{\circ}), \tag{14}$$

therefore

$$A_{brace} = \frac{V_{\mathrm{u}}}{\sqrt{2}f_y} = 2710\mathrm{mm}^2. \tag{15}$$

Further, cross-section area of inverted-V brace is 1600 mm^2. The total materials volume for every brace is same and increases 8.7%, which are presented in Table 2.

Perfect elastic-plastic model is adopted in constitutive relation of steel. The yielding stress for steel frame is 345 Mpa, and for the brace is 235 Mpa. Furthermore, elements for brace, beam and column are realized by Brace, FEMA Beam and FEMA Column in software Perform-3D. P-Δ effects is taken into account for column element. Mass is 31.05 ton in every beam-column joint. Live load is 3.0 KN/m^2, and dead load is 10.0 KN/m^2. Thus analytical models are established. The seven records of ground motion are employed in Table 3. The peak ground acceleration and damp ratio based on Code GB50011 (2010) are presented in Table 4.

In order to verify the model in software Perform-3D, software Opensees (PEER 2013) is used to compare. Thus, the first three periods of original frame are presented in Table 5. The maximum

Table 6 Comparison for the first period in Perform-3D

Configurations	Original frame	Optimized brace	Inverted "V" brace	Single-bar brace
First period (s)	2.57	1.25	1.30	1.49
Reduction (%)	--	51.4	49.4	42.0

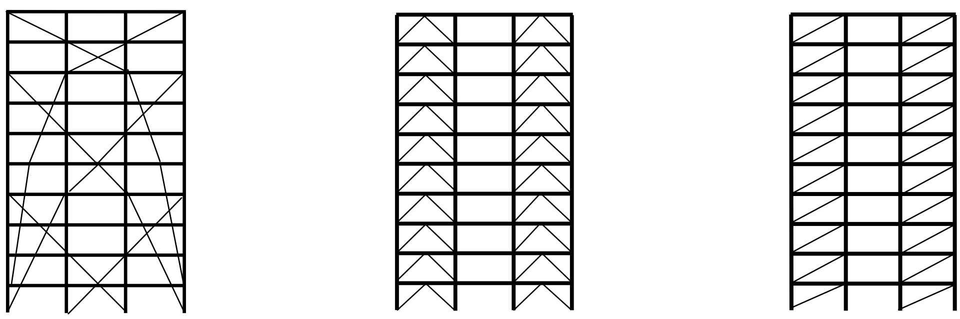

(a) Optimized brace (b) Inverted "V" brace (c) Single bar brace

Fig. 6 Brace configuration

Table 7 Mean reduction of drift under minor earthquakes

Story	Optimized brace (%)	Inverted “V” brace (%)	Single-bar brace (%)
1	5.88	17.65	11.76
2	35.71	32.14	32.14
3	42.86	28.57	28.57
4	50.00	33.33	30.00
5	41.38	31.03	31.03
6	46.43	32.14	28.57
7	40.00	32.00	28.00
8	54.17	33.33	29.17
9	50.00	27.78	22.22
10	38.46	23.08	15.38
Average	40.49	29.11	25.69

Table 8 Mean reduction of drift under rare earthquakes

Story	Optimized brace (%)	Inverted “V” brace (%)	Single-bar brace (%)
1	49.34	51.97	33.55
2	53.77	52.26	37.19
3	58.50	57.00	41.50
4	59.30	60.30	44.72
5	48.47	60.12	47.24
6	51.85	59.26	46.67
7	59.48	56.03	47.41
8	67.65	52.94	46.08
9	64.38	42.47	35.62
10	52.17	26.09	19.57
Average	56.49	51.84	39.95

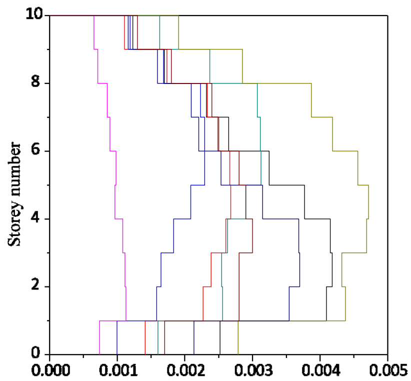

(a) Drifts of original structure

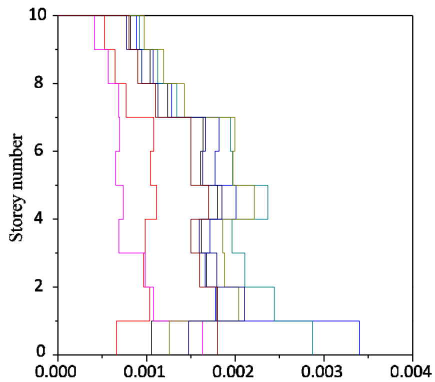

(b) Drifts of optimized brace

Fig. 7 Drifts of minor earthquakes

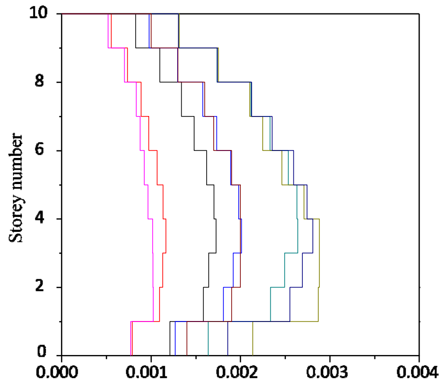

(c) Drifts of inverted "V" brace

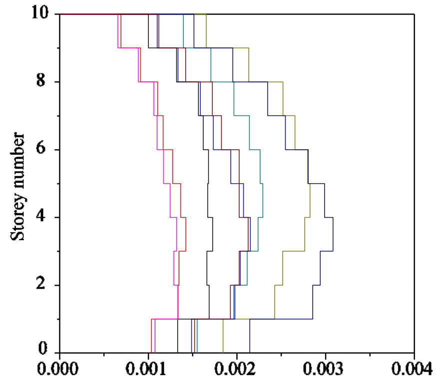

(d) Drifts of single-bar brace

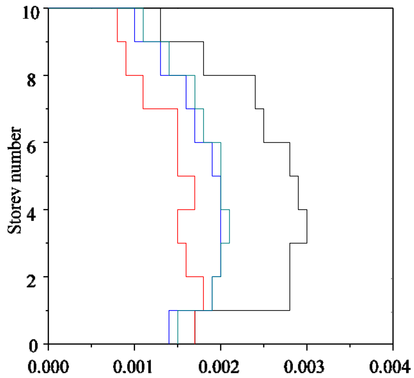

(e) Mean drifts of minor earthquakes

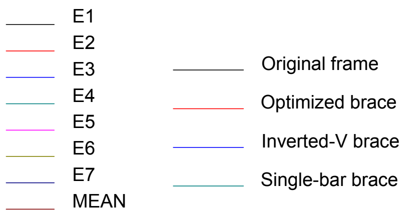

Fig. 7 Continued

deviation is 2.7% to first period in Table 5. Further, the first period of per structure is established in Table 6. The first period can be decreased using braces in Table 6.

3.3.2 Seismic analysis under minor earthquake

The story drifts are derived under minor earthquakes for every structure when peak ground acceleration is 70 cm/s^2 (including Original structure, Optimized brace, Inverted "V" brace, Single-bar brace), which are demonstrated in Figs. 7(a)-(d). The mean drift of minor earthquakes for every structure is presented in Fig. 7(e).

All structures are elastic under minor earthquakes. Fig. 7(e) demonstrates the drifts of structures with braces are less than the original one. The reduction of drifts for minor earthquakes are derived in Table 7. The reduction of drift for optimized brace is more efficient than the inverted "V" brace and single-bar brace, which can be demonstrated in Table 7.

3.3.3 Seismic performance analysis under rare earthquake

Similarly, the story drifts are derived under rare earthquakes for are presented in Figs. 8(a)-(d) when peak ground acceleration is 400 cm/s^2. The mean drifts of rare earthquakes for every structure are demonstrated in Fig. 8(e).

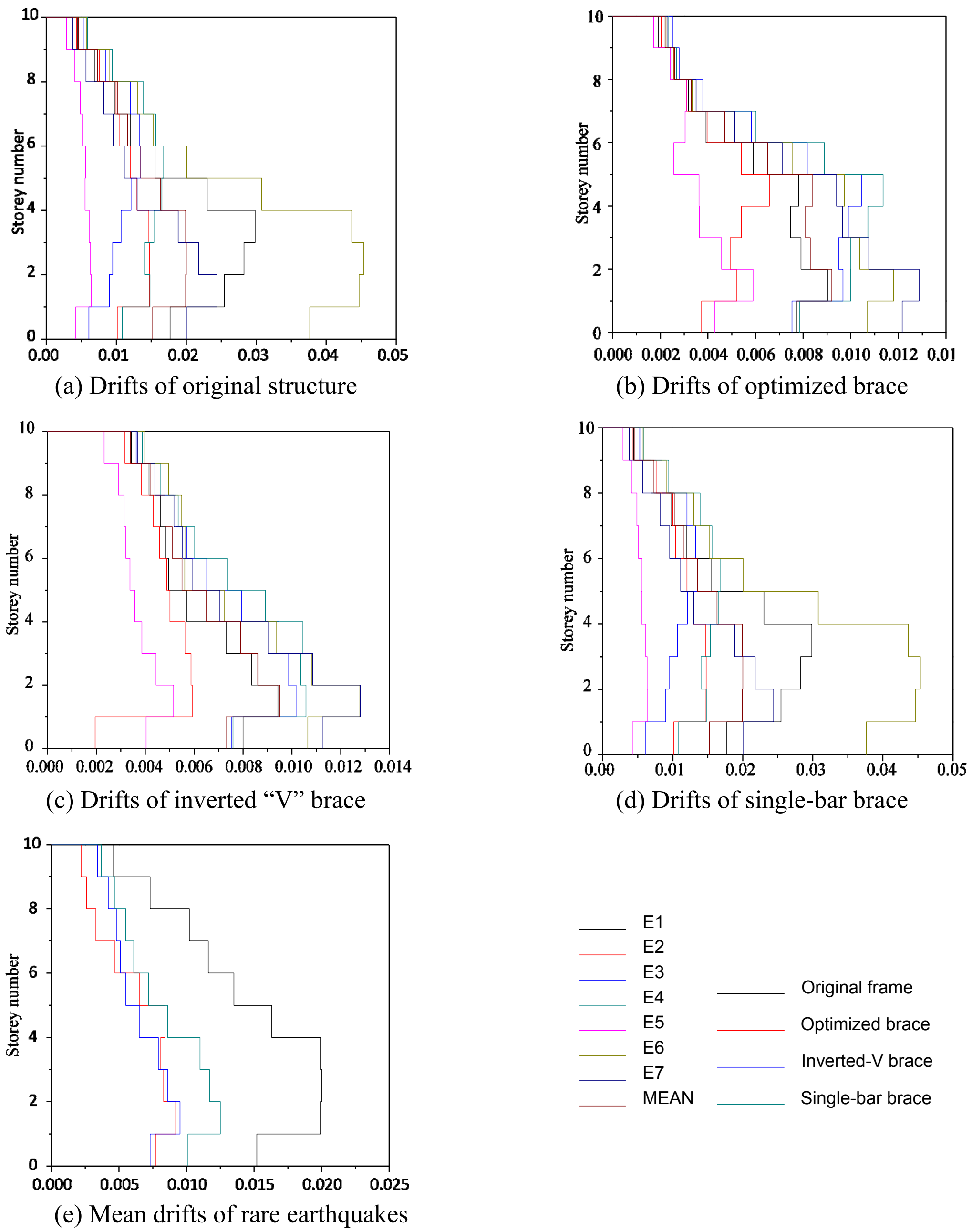

(a) Drifts of original structure

(b) Drifts of optimized brace

(c) Drifts of inverted “V” brace

(d) Drifts of single-bar brace

(e) Mean drifts of rare earthquakes

Fig. 8 Drifts of rare earthquakes

The reduction of drifts for rare earthquakes are established in Table 8. The similar reduction tendency under rare earthquakes is showed in Table 8. The reduction of drift for optimized brace is more acceptable than others, which can be showed in Table 8. Moreover, the common inverted “V” brace is not optimized. While the inverted “V” brace is more acceptable than the single-bar brace because span is twice as much as story height within every bay for this structure, which is

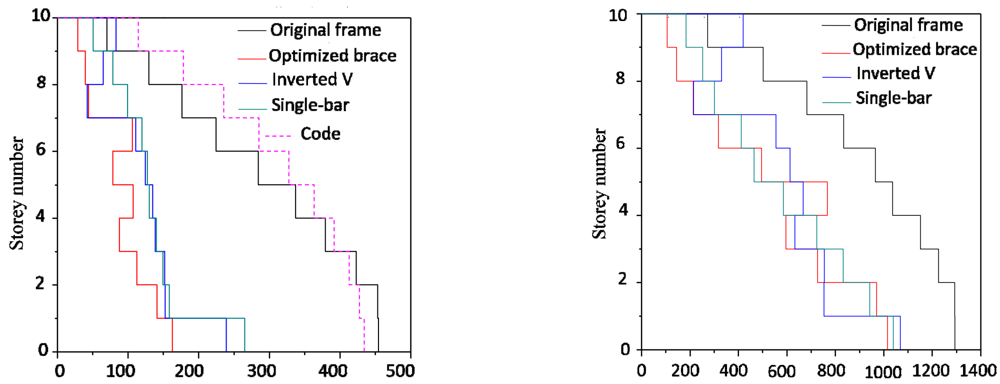

(a) Total storey shear of columns under minor earthquake E1 (KN)

(b) Total storey shear of columns under rare earthquake E1 (KN)

Fig. 9 Total storey shear of columns

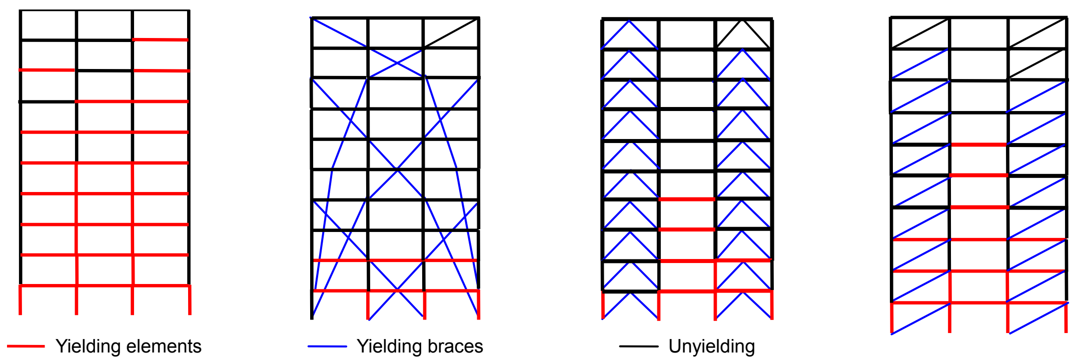

(a) Original brace (b) Optimized brace (c) Inverted "V" brace (d) Single bar brace

Fig. 10 Yielding mechanism

consistent with the results of optimized analysis.

Total storey shear of columns under minor and rare earthquake E1 are depicted in Figs. 9(a)-(b), not including the braces. The total shear of columns is reduced using braces herein. Further, yielding mechanism under rare earthquake E1 is demonstrated in Fig. 10. Beams first yield in original structure presented in Fig. 10(a), whereas braces yield firstly in structures with braces. More beams and columns yield in Fig. 10(a), therefore, brace can mitigate seismic damage.

4. Conclusions

Seismic analysis of steel structure with brace configuration using topology optimization is discussed in this paper. Further, two common braces configuration are used to compare. Some conclusions can be presented as follows.

- The optimal bracing system based on truss-like material model avoids numberical instability and shows more details for brace configuration.

- The common “X” brace and inverted “V” brace are not always optimal. Moreover, the inverted “V” brace is more acceptable than the single-bar brace when span is twice as much as story height.
- The frame structures with optimized braces are more efficient to reduce the drifts. Further, beams first undergo yielding in original steel structure, nevertheless, braces yield firstly in structures with braces. Moreover, brace can mitigate seismic damage.

Acknowledgments

The research described in this paper was financially supported by the Natural Science Foundation of China (Granted No. 51378221, 11572131), the State Key Laboratory of Subtropical Building Science Foundation of SCUT (Granted No. 2014ZC16, No 2015ZA05) and Guangzhou science and technology projects (Granted No. 15020088).

References

Abdollahzadeh, G. and Abbasi, M. (2015), “Response modification factor of suspended zipper braced frames”, *Steel Compos. Struct., Int. J.*, **18**(1), 165-185.

ASCE (2013), Seismic Evaluation and Retrofit Rehabilitation of Existing Building, American Society of Civil Engineers, Reston, VA, USA.

ASCE (2006), Seismic Rehabilitation of Existing Building, American Society of Civil Engineers, Reston, VA, USA.

AISC341-10 (2010), Seismic Provision for Structure Steel Buildings, American Institute of Steel Construction, Chicago, IL, USA.

Aydin, E., Sonmez, M. and Karabork, T. (2015), “Optimal placement of elastic steel diagonal braces using artificial bee colony algorithm”, *Steel Compos. Struct., Int. J.*, **19**(2), 349-368.

Bendsøe, M.P. and Kikuchi, N. (1988), “Generating optimal topologies in structural design using a homogenization method”, *Comput. Method. Appl. Mech. Eng.*, **71**(2), 197-224.

Computer and Structures, Inc. (2008), Perform 3D User’s Guide, CSI, CA, USA.

D’Aniello, M., La, M.A.G., Portioli, F. and Landolfo, R. (2013), “Modelling aspects of the seismic response of steel concentric braced frames”, *Steel Compos. Struct., Int. J.*, **15**(5), 539-566.

GB50011 (2010), Code for Seismic Design of Buildings, Architecture Industry Press, Beijing, China.

Ghowsi, A.F. and Sahoo, D.R. (2015), “Fragility assessment of buckling-restrained braced frames under near-field earthquakes”, *Steel Compos. Struct., Int. J.*, **19**(1), 173-190.

Jia, M.M., Lu, D.G., Guo, L.H. and Sun, L. (2014), “Experimental research and cyclic behavior of buckling-restrained braced composite frame”, *J. Construct. Steel Res.*, **95**, 90-105.

Lee, D.K., Shin, S., Lee, J.H. and Lee, K. (2015), “Layout evaluation of building outrigger truss by using material topology optimization”, *Steel Compos. Struct., Int. J.*, **19**(2), 263-275.

Lian, M., Su, M.Z. and Guo, Y. (2015), “Seismic performance of eccentrically braced frames with high strength steel combination”, *Steel Compos. Struct., Int. J.*, **18**(6), 1517-1539.

Liang, Q.Q., Xie, Y.M. and Steven, G.P. (2000), “Optimal topology design of bracing systems for multistory steel frames”, *J. Struct. Eng.*, **126**(7), 823-829.

Mijar, A.R., Swan, C.C., Arora, J.S. and Kosaka, I. (1998), “Continuum topology optimization for concept design of frame bracing systems”, *J. Struct. Eng.*, **124**(5), 541-550.

Opensees (2013), Open System for Earthquake Engineering Simulation, Pacific Earthquake Engineering Research Center, University of California, Berkeley, CA, USA. http://opensees.-berkeley.edu

Qu, Z., Maidac, Y., Sakatab, H. and Wada, A. (2015), “Seismic responses of reinforced concrete frames with buckling restrained braces in zigzag configuration”, *Eng. Struct.*, **105**(12), 12-21.

Rezvani, F.H. and Asgarian, B. (2014), “Effect of seismic design level on safety against progressive collapse of concentrically braced frames”, *Steel Compos. Struct., Int. J.*, **16**(2), 135-156.
Tasbihgoo, F., Lin, C.M. and Ho, L. (2009), “Seismic rehabilitation of Santa Monica Place Mall based on ASCE41”, *ATC&SEI Conference on Improving the Seismic Performance of Existing Buildings and Other Structures*, San Francisco, CA, USA, December.
Tirca, L., Serban, O., Lin, L., Wang, M. and Lin, N. (2015), “Improving the seismic resilience of existing braced-frame office buildings”, *J. Struct. Eng.*, **141**(7), (C4015003)1-14.
Xie, Y.M. and Steven, G.P. (1993), “A simple evolutionary procedure for structural optimization”, *Comput. Struct.*, **49**(5), 885-896.
Zhou, K.M. and Li, X. (2005), “Topology optimization of structures under multiple load cases using a fiber-reinforced composite material model”, *Comput. Mech.*, **38**(5), 163-170.
Zhou, K.M. and Chen, C.H. (2014), “Topology optimization of frame bracing system for natural frequency”, *Open Civil Eng. J.*, **8**(1), 250-256.
Zhu, M., Yang, Y., Gaynor, A. and Guest, J. (2014), “Considering constructability in structural topology optimization”, *Structures Congress*, Boston, MA, USA, April.

CC